

The classic P300 encodes a build-to-threshold decision variable



Deirdre M. Twomey,¹ Peter R. Murphy,² Simon P. Kelly³ and Redmond G. O'Connell¹

¹Trinity College Institute of Neuroscience, Lloyd Building, Trinity College Dublin, Dublin 2, Ireland

²Department of Psychology and Leiden Institute for Brain and Cognition, Leiden University, Leiden, The Netherlands

³Department of Biomedical Engineering, City College of the City University of New York, New York, NY, USA

Keywords: drift diffusion model, EEG, ERP, P300, perceptual decision-making

Abstract

The P300 component of the human event-related potential has been the subject of intensive experimental investigation across a five-decade period, owing to its apparent relevance to a wide range of cognitive functions and its sensitivity to numerous brain disorders, yet its exact contribution to cognition remains unresolved. Here, we carry out key analyses of the P300 elicited by transient auditory and visual targets to examine its potential role as a 'decision variable' signal that accumulates evidence to a decision bound. Consistent with the latter, we find that the P300 reaches a stereotyped amplitude immediately prior to response execution and that its rate of rise scales with target detection difficulty and accounts for trial-to-trial variance in RT. Computational simulations of an accumulation-to-bound decision process faithfully captured P300 dynamics when its parameters were set by model fits to the RT distributions. Thus, where the dominant explanatory accounts have conceived of the P300 as a unitary neural event, our data reveal it to be a dynamically evolving neural signature of decision formation. These findings place the P300 at the heart of a mechanistically principled framework for understanding decision-making in both the typical and atypical human brain.

Introduction

The centroparietal P300 (alternatively labelled 'P3' or 'P3b') is a large-amplitude positive event-related potential (ERP) component which peaks at ~ 300–600 ms following the presentation of any task-relevant stimulus, regardless of its sensory modality (Nieuwenhuis *et al.*, 2005; Polich & Criado, 2006; Nolan *et al.*, 2012). This component has drawn relentless interest since its initial discovery in 1965 (Sutton *et al.*, 1965) due to its apparent relevance to a wide variety of cognitive operations and its disruption in a number of prominent brain disorders (Polich *et al.*, 1990; Santosh *et al.*, 1994; Mavrogiorgou *et al.*, 2002; Prox *et al.*, 2007; Verleger *et al.*, 2013). However, despite intensive investigation, a consensus regarding the precise functional significance of the P300 has failed to emerge. Numerous explanatory accounts have been proposed, variously implicating the encoding of stimulus significance (Kutas *et al.*, 1977), decision confidence (Hillyard *et al.*, 1971; Squires *et al.*, 1973), uncertainty or surprise (Duncan-Johnson & Donchin, 1977; Mars *et al.*, 2008), or asserting a role in context updating (Donchin & Coles, 1988), neuroinhibition (Polich, 2007), event-categorization (Kok, 2001), orienting and response potentiation (Nieuwenhuis *et al.*, 2005, 2011) or context closure (Verleger, 1988). However, no single model has received conclusive empirical validation and this lack of clarity has greatly limited the P300's utility as an interpretable neurocognitive marker in both basic and clinical research.

Early research on the P300 systematically examined its sensitivity to variations in perceptual performance within a signal detection framework (Hillyard *et al.*, 1971; Squires *et al.*, 1973). These studies established that the P300 is larger when evoked by detected versus undetected stimuli, that its peak latency varies with RT, and that it is sensitive to experimental manipulations impacting on stimulus evaluation. This initially prompted a view that the P300 was linked in some way to the neural process through which sensory information is translated into adaptive action, i.e., perceptual decision-making (Smith *et al.*, 1970; Rohrbaugh *et al.*, 1974), but whether and how the P300 might itself contribute to forming decisions was never established. Today, the two most influential accounts of the P300 (Donchin & Coles, 1988; Nieuwenhuis *et al.*, 2005) propose that it has no direct role in decision formation but reflects a process that is triggered by the outcome of decision making. However, in recent years our understanding of the neural mechanisms underpinning perceptual decision making has expanded through a combination of mathematical modelling and single-unit recording studies (Smith & Vickers, 1988; Smith & Ratcliff, 2004; Gold & Shadlen, 2007; Shadlen & Kiani, 2013). A key insight from this work is that perceptual decisions arise from a process of sequential sampling and accumulation of sensory evidence, and models founded on these principles offer a clear set of empirically verifiable predictions regarding the dynamics that a neural decision variable signal should exhibit. Here, we conduct a series of critical analyses to verify the extent to which each of these predictions is met by the classically-evoked P300 using data from oddball and target detection paradigms.

Correspondence: Dr Redmond G. O'Connell, as above.

E-mail: reoconne@tcd.ie

Received 9 February 2015, revised 3 April 2015, accepted 24 April 2015

Materials and methods

In order to comprehensively probe the P300's role in decision formation we analysed data from three experiments, each of which involved separate participant samples and employed a distinct target detection paradigm (four-stimulus auditory oddball, two-stimulus auditory oddball and visual target detection task).

Participants

Fifteen participants completed the four-stimulus auditory oddball experiment. One was excluded due to poor accuracy (detection accuracy < 50%), yielding a final sample of 14 participants (five male, two left-handed), with a mean age of 29 years (SD = 5.8). The two-stimulus auditory oddball sample consisted of 33 participants with five excluded due to excessive artifacts in the electroencephalography (EEG) data (< 50 trials remaining), yielding a final sample of 28 participants (13 male, two left-handed), with a mean age of 23.1 years (SD = 4.2). Fifteen participants (six female, one left-handed), with a mean age of 21.7 years (SD = 4.3) completed the visual target detection paradigm. All participants had normal or corrected-to-normal vision, no history of psychiatric illness or head injury, and provided written informed consent in advance of testing. All procedures were approved by the Trinity College Dublin ethics committee and in accordance with the Declaration of Helsinki.

Experimental tasks

The four-stimulus auditory oddball stimuli were presented through headphones using the Presentation software suite (NeuroBehavioural Systems, San Francisco, CA, USA) and consisted of sinusoidal tones of 60 ms duration. Participants were instructed to make a speeded right index finger mouse click to target tones (either 530, 590 or 680 Hz, 6.7% of trials each) while ignoring the presentation of non-target tones (500 Hz). A total of 1500 tones were presented with an interstimulus interval (ISI) that varied pseudorandomly between 1 and 2 s. The stimuli were ordered such that at least two non-target tones were presented between targets, leaving a minimum inter-target interval of 3 s. Participants completed a practice session to ensure they were well acquainted with the instructions prior to beginning and were seated at a distance of ~50 cm from a 20-inch LED monitor (Dell P2011H; Dell Inc., Ireland) with their head supported by a chin rest. Participants completed ten 3.5-min blocks of the task.

Task instructions and testing conditions in the two-stimulus auditory oddball experiment were identical to those in the four-stimulus auditory oddball experiment (see Murphy *et al.*, 2011). However, the targets were 1-kHz tones while the non-target tones were presented at 500 Hz. The targets were pseudorandomly distributed throughout the task and comprised 20% of the total number of trials. A total of 890 tones were presented with an ISI that varied pseudorandomly between 2.1 and 2.9 s. The stimuli were arranged such that at least three non-target tones separated the targets, leaving a minimum inter-target interval of 8 s. The total duration of the task was 37 min with no breaks.

The visual target detection experiment was conducted as part of a separate study (O'Connell *et al.*, 2012). Participants were seated ~50 cm from an LCD monitor with a 120-Hz frame rate, and made a speeded button press to transient (100 ms) size increases (from an initial five pixels to a target of 10 pixels) in a white central fixation square that was continuously presented for 4 min at a time. For reasons not relevant to the present experiment (see O'Connell *et al.*, 2012), the fixation square was surrounded by a 20-Hz flickering annular pattern (inner radius 1.14°, outer radius 3.1°) that consisted

of light and dark radial segments that alternated with two cycles per quadrant. The annulus underwent periodic task-irrelevant decreases in contrast (from 65 to 35% over 1.6 s) and participants were instructed to ignore the annulus at all times (data presented in O'Connell *et al.*, 2012 indicate that this instruction was obeyed). Between 23 and 27 fixation targets were presented per block at random times following each contrast change. Participants completed two blocks of the task. O'Connell *et al.* (2012) demonstrated that the visual targets elicited a typical P300 component; here, we present a novel set of analyses that were not reported in that paper.

Data acquisition and preprocessing

Continuous EEG data were acquired using an ActiveTwo system (BioSemi, The Netherlands) from 128 scalp electrodes (64 electrodes in two-stimulus auditory oddball experiment) and digitized at 512 Hz. In all three experiments, vertical and horizontal eye movements were recorded using two vertical electro-oculogram (EOG) electrodes placed above and below the left eye and two horizontal electrodes placed at the outer canthus of each eye, respectively. Data were analysed using custom scripts in MATLAB (Mathworks, Natick, MA, USA), drawing on EEGLAB (Delorme & Makeig, 2004) routines for reading in data files and spherical spline interpolation of noisy channels. EEG data were re-referenced offline to the average reference and low-pass filtered below 35 Hz using a direct form II second-order Butterworth infinite impulse response filter. The 'filtfilt' function in MATLAB was implemented to allow for a non-causal zero-phase filtering approach, which would have eliminated any nonlinear phase distortion associated with the use of an infinite impulse response filter. No high-pass filter was applied either on- or offline. Trials were rejected if the bipolar vertical EOG signal (upper minus lower) exceeded an absolute value of 200 μ V or if any scalp channel exceeded 100 μ V at any time during the epoch.

EEG data were segmented into epochs centred on target onset using windows of -500 to 1500 ms (four-stimulus oddball), -500 to 1200 ms (two-stimulus oddball) and -500 to 1250 ms (visual target detection) relative to target onset. The epochs were then baseline-corrected relative to the 100-ms interval prior to target onset in the two- and four-stimulus auditory oddball experiments and relative to the 500 ms prior to target onset in the visual target detection experiment. In all three experiments, response-aligned traces were derived by extracting epochs from -500 to 50 ms relative to the response on each trial. P300 amplitude and build-up rate were measured from electrodes centred on the region of maximum positive amplitude identified in the grand average scalp topography for each experiment; depending on the montage density and focus, a similar spatial area encompassed a varying number of electrodes (four-stimulus oddball, cluster of four electrodes anterior to Pz; two-stimulus oddball, electrode Pz; visual target detection experiment, cluster of six electrodes centred on Pz). All single-trial EEG data were converted to current source density (CSD; Kayser & Tenke, 2006) to counteract spatial overlap between the P300 and a functionally distinct frontocentral negativity (see Data S1 and Kelly & O'Connell, 2013).

Signal analysis

Traditionally the P300 has been measured in terms of its peak amplitude and latency in the stimulus-aligned average waveform. However, sequential sampling models and primate electrophysiology offer detailed predictions regarding the dynamics that a decision variable signal should exhibit that call for a more comprehensive analysis of the P300 waveforms as described below.

A build-up rate that scales with the strength of sensory evidence and predicts RT

A strong prediction of sequential sampling models is that the build-up rate of a decision variable signal should scale with the strength of sensory evidence, consistent with temporal integration. A further prediction is that RT variability results in large part from variation in the build-up rate of the decision variable, either across trials (Reddi & Carpenter, 2000; Brown & Heathcote, 2008), within trials (Link & Heath, 1975; Palmer *et al.*, 2005) or both (Ratcliff & McKoon, 2008), even when the sensory evidence has identical statistics across trials. We first examined the extent to which the build-up rate of the P300 scales with evidence strength using data from the four-stimulus auditory oddball task which incorporates three distinct levels of target discrimination difficulty. Following the application of artifact rejection procedures the average numbers of target trials remaining for each participant, per level of target detection difficulty, were (mean \pm SD): 530 Hz, 76.3 \pm 18.8; 590 Hz, 89.9 \pm 9.3; 680 Hz, 88.7 \pm 11.1. The build-up rate of the P300 was measured as the slope of a straight line fitted to the unfiltered stimulus- and response-aligned ERP waveforms for each target type.

To conduct a detailed test of the influence of P300 build-up rate on detection times when evidence is held constant, we analysed previously collected data from a two-stimulus auditory oddball task that was continuously performed for \sim 38 min (Murphy *et al.*, 2011), thus ensuring that there was substantial trial-to-trial variability in RT. Using the auditory oddball data we split each participant's RT distribution into equal-sized fast, medium and slow RT bins and plotted the grand average signal time courses aligned to both the target onset and response execution for each bin (Fig. 1B). Following artifact rejection, a mean number of 46 (SD = 9.4) target trials remained per participant per RT bin. To verify whether any relationships between the P300 and decision making were modality-independent we conducted a similar analysis of the visual target detection dataset. As there were fewer trials available for analysis in the visual target detection experiment, each participant's RT distribution was divided into two equal-sized fast and slow bins based on a median split. Across participants a mean number of 21 target trials (\pm 2.2) remained in each RT bin, following the application of artifact rejection procedures.

The time intervals used for P300 slope measurement were as follows: stimulus-aligned P300 slope was measured across intervals of 200–350 ms in the two- and four-stimulus auditory oddball experiments respectively. The slope of the response-aligned P300 was measured across a window of -250 to 0 ms centred on response execution in the two-stimulus auditory oddball and visual detection experiments. A smaller interval of -250 to -50 ms centred on response execution was used to measure the build-up rate of the P300 in the four-stimulus auditory oddball experiment due to the observed conversion of build-up rates immediately prior to response execution (see section 3.4 and Fig. 1A). To enable a finer characterization of the signal dynamics and their relationship to RT in the two-stimulus oddball data, we isolated single-trial measures of ERP slope and amplitude relative to decision report. The single-trial data were de-noised using a 20-Hz low-pass filter.

An action-triggering threshold

An additional defining feature of a decision variable signal in the context of RT tasks is that it reliably triggers action upon reaching a fixed threshold level. We verified whether the P300 exhibits such character-

istics using all three datasets. The threshold-crossing effect is most appropriately tested on the variance of peak amplitude at response-aligned waveforms, which should, theoretically, be zero for an accumulation process with a fixed threshold in the absence of measurement and background neural noise (see Fig. 1A). However, as the dominant approach in the literature has been to measure the P300 relative to stimulus onset, we also examined the RT–threshold relationship in the stimulus-aligned waveforms to allow for a direct comparison with previous studies. The peak amplitude of the P300 was defined as the largest positive peak within an appropriate interval in the stimulus- and response-aligned traces based on inspection of the grand-average waveforms. In the stimulus-aligned averages, P300 amplitude was measured across time windows of 300–550, 310–420 and 300–450 ms in the four-stimulus oddball, two-stimulus oddball and the visual target detection experiments respectively. In the response-aligned average, the peak amplitude of the P300 was measured across a -30 to 0 ms interval centred on response execution in all three experiments. As a further test of the threshold-crossing effect on RT, we compared trial-to-trial variance in P300 amplitude measured immediately in advance of response initiation (-100 to 50 ms) in the two-stimulus auditory oddball data, to a null distribution of the same variance metric computed when RTs were randomly re-assigned to trials. Five hundred permutations were used for each individual subject, and variance values were calculated for P300 amplitudes in bins of five trials, grouped after trials were sorted in order of ascending RT. These values were representative of the values obtained for larger bin sizes (Fig. S1). The variance metric for the unshuffled data was then expressed as a z -score with respect to the null distribution for each subject, and these z -scores were tested against zero.

Comparison with simulated decision variable

To further illustrate how P300 dynamics can be explained by a decision variable process that accumulates noisy sensory evidence to a fixed decision bound, we fitted a reduced diffusion model to the RT distributions of the four-stimulus auditory oddball task and simulated the resultant mean decision variable trajectories over time (Fig. 2A). RT data for each of the three oddball difficulty levels in the four-stimulus auditory oddball experiment were pooled across subjects. As misses were few and depended on the variable inter-target interval these trials were omitted from the model fit for simplicity, thus leaving just the trials that contribute to the stimulus- and response-locked P300 waveforms. The model was fitted to all data at once, and included a constant non-decision time component T_{er} accounting for delays due to processes other than the evidence accumulation process, a within-trial noise parameter s which quantified the SD of a Gaussian noise process comprising the sole source of within-condition, across-trial variability in RT, and drift rate parameters v_1 , v_2 and v_3 , one for each of the three oddball difficulty levels. Thus, there were five free parameters in total and only drift rate was allowed to vary across difficulty levels. The decision bound a was a scaling parameter, fixed at a value of 1 for all conditions. The fit was performed by minimizing a χ^2 error statistic using a bounded simplex algorithm. We simulated the same number of trials as in the real data, in each of which a random diffusion process with the best-fit parameters from the behavioural fit and approximately the same 2-ms temporal resolution as the EEG was played out from T_{er} until reaching the decision bound a . To enable comparison with the ERP data, it was necessary to additionally model the return path of the decision variable from bound to starting point after each bound-crossing. For this we implemented a gradual decay back to baseline at a mean rate

that was fixed across all conditions and that roughly matched the post-response decline of the observed, response-locked P300.

Statistical analyses

The impact of target discrimination difficulty on the build-up rate and amplitude of the P300 was established using two separate one-way repeated-measures ANOVAs. Four separate one-way repeated-measures ANOVAs were conducted to investigate within-subject relationships between RT and the build-up rate and amplitude of the P300 in the two-stimulus oddball and visual target detection data. Furthermore, in the two-stimulus oddball data, each participant's single-trial signal slope and amplitude measures were regressed against their single-trial RT and the resulting beta values were subjected to a *t*-test against 0. Mean values are quoted \pm SD. Where ANOVAs were used for statistical analyses and sphericity was violated in factors with two or more levels, the Greenhouse–Geisser or the Huynh–Feldt corrected degrees of freedom are reported (the correction applied was contingent on the degree of violation).

Results

Behaviour

As expected, in the four-stimulus auditory oddball the manipulation of target detection difficulty had a significant impact on both

detection accuracy ($F_{1,13} = 6.7$, $P = 0.02$: 530 Hz target, $87.1 \pm 17.5\%$; 590 Hz targets, $99.4 \pm 1.1\%$; 680 Hz targets, $99.8 \pm 0.056\%$) and RT ($F_{1,3,16.4} = 73.7$, $P = 0.0001$: 530 Hz targets, 533.3 ± 50.9 ms; 590 Hz targets, 455.2 ± 43.9 ms; 680 Hz targets, 416.6 ± 44.3 ms). Targets in the two-stimulus-oddball were rarely missed (accuracy, $99.7\% \pm 0.9$) and RTs were 460.9 ± 107.7 ms. Visual targets were detected with $100 \pm 0\%$ accuracy, a mean RT of 366 ± 23 ms and 0.05 ± 0.26 false alarms.

In the following set of analyses we examined the extent to which the classic P300 bears the defining characteristics of a decision variable signal as predicted by mathematical models and primate neurophysiology.

A build-up rate that scales with the strength of sensory evidence

The grand average signal time courses aligned to target onset and response execution were plotted for each level of target detection difficulty in the four-stimulus oddball data (Fig. 1A). The build-up rate of the P300, which was measured as the slope of a straight line fitted to the unfiltered ERP waveform of each participant, increased in proportion to the strength of sensory evidence, such that stronger sensory evidence was associated with a steeper rate of rise. This effect was significant in both the stimulus ($F_{2,26} = 4.8$, $P = 0.02$) and the response-aligned traces ($F_{2,26} = 3.8$, $P = 0.04$; Fig. 1A).

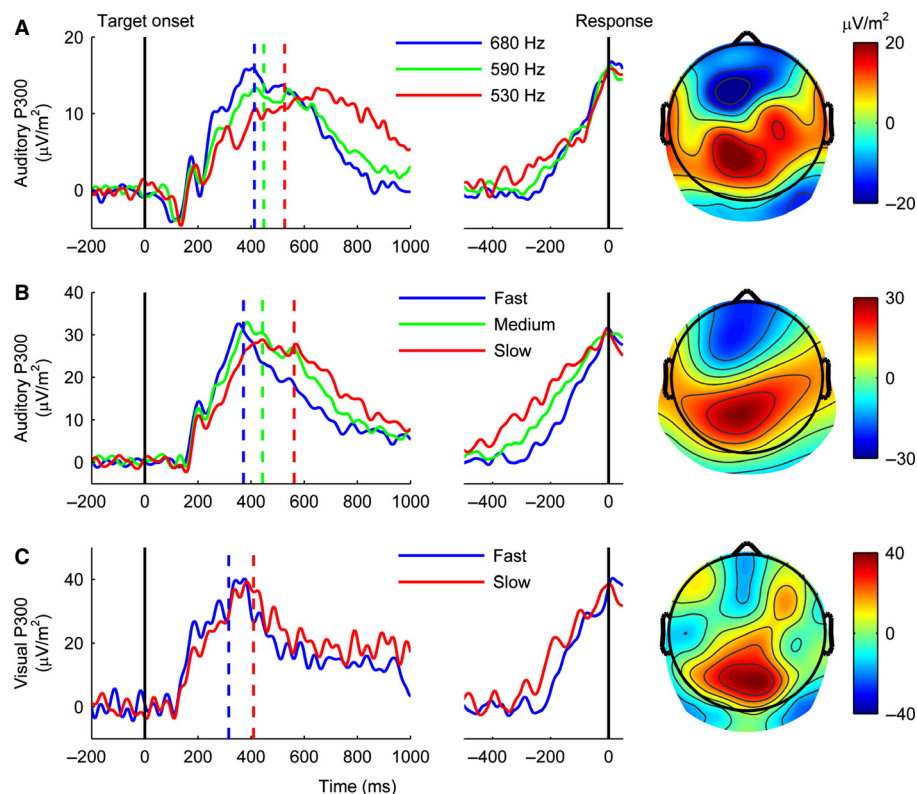


FIG. 1. The P300 exhibits the critical dynamic properties of a neural decision variable. P300 waveforms aligned to stimulus onset (left column), response execution (middle column) and signal scalp topographies across a time window of -25 to $+25$ ms centred on response execution (right column). In all panels, the coloured vertical lines denote mean RT for each condition. Single-trial EEG data were converted to CSD to minimize the projection of motor preparation signals to centroparietal electrodes. (A) The build-up rate of the response-aligned P300 in the four-stimulus auditory oddball task increased in proportion to the strength of sensory evidence (oddball pitch above non-target tone), consistent with temporal integration. (B) In the two-stimulus auditory oddball task, the response-aligned auditory P300 for three equal-sized RT bins exhibited a gradual build-up rate that scaled with RT and reached a stereotyped zenith at response execution. (C) In the visual target detection paradigm, the response-aligned visual P300 for two equal-size RT bins exhibited equivalent accumulation-to-bound dynamics to those observed in B, confirming the supramodal nature of the P300.

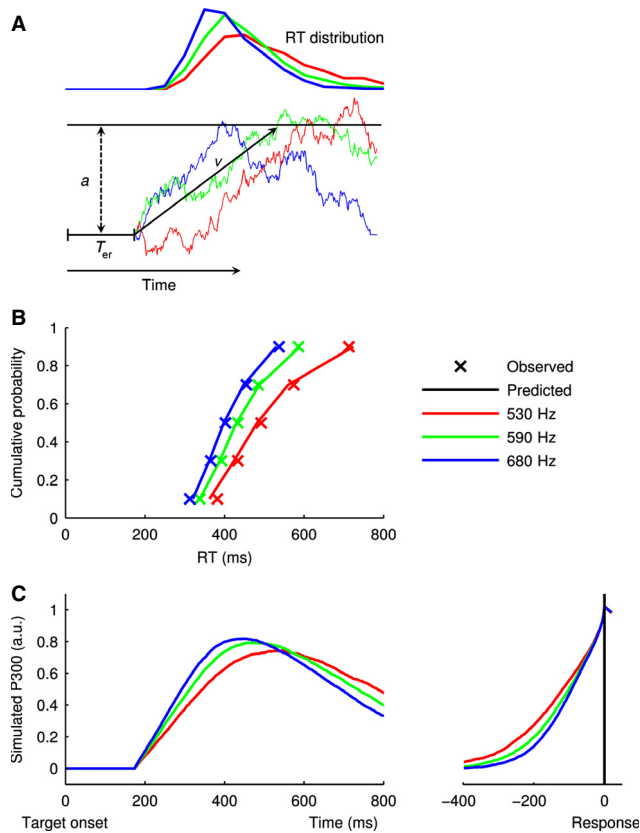


Fig. 2. Computational modelling of an accumulation-to-bound decision process captures oddball performance and P300 dynamics. (A) Three sample paths of the modelled decision process (bottom) and RT histograms from the four-stimulus auditory oddball task (top). For each target difficulty level, noisy evidence is accumulated at a mean rate that is parameterized by drift rate (v) and a detection response is triggered when the path reaches the decision bound. In order to facilitate modelling of the neural waveforms, the process does not terminate upon reaching the bound but, subject to the ongoing within-trial-noise, returns gradually to baseline at a fixed rate. (B) Predicted and observed RT quantiles for each of the three target difficulty levels. (C) Simulated decision variable waveforms aligned to target (left) and response (right) onset.

A build-up rate that predicts RT

To examine the relationship between P300 build-up rate and RT, we split each participant's RT distribution into equal-sized fast, medium and slow RT bins and plotted the grand average signal time-courses aligned to both the target onset and response execution for each bin (Fig. 1B) in the two-stimulus oddball data. Consistent with a decision variable signal, the slope of the response-aligned P300 reliably differentiated RT bins such that faster build-up was associated with faster RTs ($F_{2,54} = 8.8$, $P = 0.001$; Fig. 1B). In a further analysis, we regressed single-trial measurements of P300 build-up rate onto RT for each subject and a t -test revealed that the resultant beta weights were significantly more negative than would be expected by chance ($t_{27} = -4.02$, $P = 0.0001$).

An action-triggering threshold

Analysis of the response-aligned traces in the two-stimulus auditory oddball task revealed that P300 peak amplitude did not vary as a function of RT bin in the grand average ($F_{2,54} = 0.1$, $P = 0.9$) or at the single-trial level ($t_{27} = -1.1$, $P = 0.3$). Furthermore, trial-to-trial variance in amplitude measured immediately in advance of response

initiation was significantly lower than a permutation distribution derived by randomly reassigning RTs to trials over repeated iterations ($t_{27} = -2$, $P = 0.03$, one-tailed; Fig. S1). In contrast, the amplitude of the P300 in the stimulus-aligned average decreased as a function of RT ($F_{2,54} = 4.3$, $P = 0.02$). This effect can be explained by the fact that a signal whose peak is most precisely time-locked to the response will exhibit reduced amplitude in the stimulus-aligned average in proportion with the temporal variability of the response. Indeed, the amplitude reduction was most pronounced in the slowest RT bin, whose intra-subject variability (100.53 ± 38 ms) was substantially greater than that of the medium (19.43 ± 6.9 ms) or fast (27.89 ± 10.6 ms) bins. Analysis of the response-aligned averages in the four-stimulus oddball task also confirmed that P300 peak amplitude was insensitive to sensory evidence strength ($F_{2,26} = 0.1$, $P = 0.9$).

Inspection of the average waveforms revealed that the peak latency of the P300 coincides with response execution whereas the crossing of the decision threshold and the initiation of the response must occur some time earlier. A plausible explanation for this overshoot effect is that it reflects sensory information that had already entered the processing pipeline at the time of decision commitment (Resulaj *et al.*, 2009). This is an interesting phenomenon worthy of further investigation and there is already compelling evidence to suggest that this additional post-commitment information plays an important role in the correction or countermanding of erroneously executed actions (Resulaj *et al.*, 2009).

The P300 as a domain general decision signal

To verify the generality of the P300 dynamics identified above in the auditory domain, we sought to demonstrate equivalent build-to-threshold dynamics in the visual target detection task. Each participant's RT distribution was divided into equal-sized fast (315.7 ± 18.7 ms) and slow (409.2 ± 14.8 ms) RT bins. Despite the modest differences in mean RT across bins (Fig. 1C), the dynamics of the response-aligned visual P300 were consistent with those observed in the auditory domain: its rate of rise reliably differentiated RT bins such that a faster build-up rate resulted in faster RTs ($F_{1,14} = 7.4$, $P = 0.02$) and its peak amplitude did not vary as a function of RT ($F_{1,14} = 1.1$, $P = 0.3$; see Fig. 1C). Thus, the P300 component exhibited equivalent accumulation-to-bound dynamics across the two sensory modalities.

Comparison with simulated decision variable

We fitted a reduced diffusion model comprising five free parameters to the RT distributions of the four-stimulus auditory oddball task and simulated the resultant mean decision variable trajectories over time. This minimalistic model accounted well for the observed RT distributions (Fig. 2B). Decision variable trajectories were then simulated using the best-fitting parameter values, incorporating a gradual decline (fixed across difficulty levels) to baseline after reaching threshold. As Fig. 2C illustrates, the model waveforms recapitulate all of the key qualitative features observed in the P300 data (Fig. 1A) including (i) a build-up rate dependence on target difficulty, (ii) a stereotyped amplitude at response execution, (iii) an inverse relationship between peak amplitude in the stimulus-aligned average and target difficulty reflecting the influence of RT variability and (iv) a convergence of build-up rates across conditions for the last 100 ms prior to response execution. This last phenomenon reflects the fact that, due to high within-trial noise, the time at which the decision bound is crossed is often determined by a brief positive

signal fluctuation (see Mazurek *et al.*, 2003 for a similar result). It should be emphasized that our purpose in this modelling exercise was not to achieve a precise fit to both the behavioural and neural data, but rather to demonstrate that a model with even the bare minimum of free parameters (three for any given evidence level, compared to, for example, nine in current versions of the drift diffusion model; Vandekerckhove & Tuerlinckx, 2008), can reproduce the most salient characteristics of the P300 observed in this study.

Discussion

Our empirical data and computational modelling converge to establish that the classic P300 exhibits all of the characteristic dynamical properties of the 'decision variable' signals predicted by sequential sampling models and recently observed in primate and human electrophysiology (Shadlen & Kiani, 2013; Kelly & O'Connell, 2015): a gradual evidence-dependent build-up whose rate determines RT and a boundary-crossing effect at response execution. Our findings also suggest that the P300 reflects the same neural process as another, recently reported, human decision variable signal. When participants perform tasks that involve slow, deliberative perceptual decisions, a topographically similar but temporally extended centroparietal positivity (CPP) exhibits a gradual, evidence-dependent build-up to a fixed threshold level that precisely determines the timing and accuracy of perceptual reports across trials (O'Connell *et al.*, 2012; Kelly & O'Connell, 2013). Our study thus establishes the equivalence of the P300 and the CPP. In so doing, we also provide confirmation that the sequential sampling and accumulation of evidence is not exclusively implemented during difficult, temporally extended, discriminations necessitated by typical perceptual decision making paradigms but is equally apparent prior to rapid detections of punctate stimuli.

One of the shortcomings of sudden-onset discrete-trial presentation, which is often favoured in ERP research, is that the stimuli elicit strong early sensory-evoked components that may partly obscure the dynamics of an unfolding decision process. This is a particular concern when comparing decision-related activity across experimental conditions that affect RT because the extent of such signal overlap may vary as a function of RT. Nevertheless, the fact that the P300 exhibited a stereotyped amplitude across evidence levels and RT in the present study indicates that, although sensory-locked components are mixed in to the early part of the ERP waveforms, they do not hinder the observation of key dynamic characteristics of the decision variable. Moreover, the close correspondence between the observed P300 and the simulated decision variable waveforms provides a strong indication that interference from overlapping sensory-locked components does not account for our results.

By identifying the P300 as a neural decision variable we place it at the heart of a comprehensive theoretical framework that can account for its cardinal functional characteristics, thus calling for a reinterpretation of the prevailing explanatory accounts. Perhaps the most influential of these has been the 'context updating' hypothesis (Donchin & Coles, 1988), which proposes that the P300 reflects the revision of the current mental model of the task environment when an unexpected stimulus is identified. While this proposal is consistent with a range of key experimental effects pertaining to the P300, most notably its sensitivity to subjective probability, it rests on the assumption that the signal is only evoked after the stimulus and its probability have been evaluated. Our data directly contradict this assumption because they show that, rather than being triggered by the completion of stimulus identification, the P300 traces the identification process itself. This marks a departure from the traditional conception of ERP components as unitary processes that unfold in a

stereotyped way in relation to a discrete eliciting event, and instead highlights the important mechanistic insights that can be gleaned from the finer dynamics of their trajectories.

The decision-variable account of the P300 is novel not just in its details but more fundamentally in its nature. Whereas constructs such as context updating (Donchin & Coles, 1988) and context closure (Verleger, 1988) are qualitative ones, removed from computational realization, the sequential sampling framework is a mechanistic one that makes concrete, empirically verifiable, predictions regarding signal dynamics. For example, in addition to accounting for dynamic aspects such as the variable build-up rate and boundary-crossing effect observed here, sequential sampling models can explain the well-established inverse relationship between the amplitude of the P300 and stimulus probability. Specifically, this would reflect a strategic adjustment to the quantity of evidence required to trigger commitment to a particular decision (i.e. the start-to-threshold distance) in accordance with prior information (Smith & Vickers, 1988; Smith & Ratcliff, 2004). Another influential and more mechanistic theory has been that the P300 is a cortical manifestation of the phasic locus-coeruleus/noradrenergic (LC/NE) orienting and response potentiation (Nieuwenhuis *et al.*, 2011). This hypothesis is drawn primarily from the observation of numerous similarities in the antecedent conditions that drive the LC/NE phasic response and the P300, as well as evidence from pharmacological (Glover *et al.*, 1988; Pineda & Westerfield, 1993; Swick *et al.*, 1994; Pineda *et al.*, 1997) and pupillometric studies (Friedman *et al.*, 1973; Murphy *et al.*, 2011). However, as with context updating, a core component of this model is that the orienting response, and therefore the P300, serves to facilitate neural processes that are triggered by the outcome of the decision-making process. While our data call for a very different interpretation of the P300 they do not exclude a supportive role for the LC/NE system in its potentiation (de Gee *et al.*, 2014). One long-standing proposal that our data do support is that the peak latency of the P300 indexes the duration of stimulus evaluation processes (Kutas *et al.*, 1977; Duncan-Johnson, 1981) but, for the first time, our study identifies the specific neural mechanism that underpins this relationship.

Establishing a functional equivalence with the CPP has important implications for interpreting the role of the P300 in cognition. A feature of the CPP that sets it apart from all previously reported build-to-threshold decision variable signals is that it traces decision formation in a way that is abstracted from the specific sensory or motor requirements of the task (O'Connell *et al.*, 2012). We have also shown that the build-up of the CPP reliably precedes that of motor-selective decision signals. Together, these characteristics strongly imply that the P300 and CPP serve as an intermediate step between sensory encoding and motor preparation. A possible alternative explanation of these results is that, rather than holding any information regarding the likely decision outcome, the P300 reflects the encoding of confidence which builds with accumulated evidence (Urai & Pfeffer, 2014). However, the fact that the P300 reaches a stereotyped amplitude prior to response regardless of evidence strength or RT is inconsistent with such an account as both of these factors are known to impact systematically on subjective confidence reports (Kiani & Shadlen, 2009; Yeung & Summerfield, 2012).

Consideration of the analytic methods used in previous P300 studies points to reasons why accumulation-to-bound characteristics have been overlooked. The observation that the P300 was primarily sensitive to experimental manipulations bearing on stimulus evaluation (Duncan-Johnson & Donchin, 1977; Kutas *et al.*, 1977; Duncan-Johnson, 1981; Donchin & Coles, 1988) motivated its measurement in stimulus-aligned average waveforms, an approach that has been adopted in the

overwhelming majority of studies. Our results indicate that analysis of the stimulus-aligned waveform obscures the critical boundary-crossing effect at response execution due to the impact of RT variability on the trial-averaged peak; this effect is clearly apparent for both the P300 (Fig. 1) and simulated decision variable waveforms (Fig. 2C). Another issue has been that the P300, or 'P3b,' bears spatiotemporal overlap with a distinct frontal process 'P3a' that scales with stimulus novelty. The P3a and P3b have in some instances been grouped together in terms of their hypothesized underlying mechanisms (Nieuwenhuis *et al.*, 2005) and may be difficult to tell apart particularly when tasks involve viewing of stimuli with high-level semantic content such as verbal material (Fabiani *et al.*, 1986) or emotionally valent stimuli (Keil *et al.*, 2002). While P3a/P3b overlap is not an issue in tasks with minimal novelty such as those used in the present study, the insights obtained on how P3b dynamics relate to stimulus identification and responding may be exploited in experimental designs with higher-level or more varied stimuli to facilitate separation of the two processes.

Where the P300 has traditionally been measured in terms of its peak amplitude and latency, our results highlight that it bears a number of additional parameters that have independent influences on the timing and accuracy of decisions. These include the latency of its onset, marking the start of evidence accumulation, and its rate of rise, indexing the rate of evidence accumulation. These observations have major implications for the interpretation of P300 data because they reveal that there are multiple different reasons why the stimulus-aligned P300 peak might be delayed in a particular clinical population or experimental condition: because evidence accumulation started at a later time, because evidence was accumulated at a slower and more variable rate or because of an elevated decision threshold necessitating accumulation over a longer interval. Here we show that each of these distinct parameters can be directly measured from the P300. Furthermore, by embedding the P300 within the sequential sampling framework it is possible to generate very precise and testable predictions about how each of these parameters should vary as a function of specific stimulus properties such as probability and discriminability. This paves the way for a new and more precise understanding of how clinical brain disorders and experimental manipulations impact on decision-making in the human brain.

Supporting Information

Additional supporting information can be found in the online version of this article:

Data S1. Experimental procedures.

Fig. S1. Effect of bin-size on P300 amplitude variance reduction at response time relative to a permutation distribution in the two-stimulus auditory oddball experiment (z-scores averaged across subjects).

Fig. S2. Inverse relationship between untransformed response-aligned P300 amplitude and RT is driven by a frontocentral negativity.

Acknowledgements

This study was supported by grants from the United States National Science Foundation (BCS-1358955 to S.P.K. and R.O.C.), the Irish Research Council for Science Engineering and Technology (to D.M.T. and P.R.M.) and Trinity College Dublin (to D.M.T.). The authors declare no competing financial interests. We thank Sander Nieuwenhuis for helpful discussions.

Abbreviations

CPP, centroparietal positivity; CSD, current source density; EEG, electroencephalography; ERP, event-related potential; RT, reaction time.

References

- Brown, S.D. & Heathcote, A. (2008) The simplest complete model of choice response time: linear ballistic accumulation. *Cognitive Psychol.*, **57**, 153–178.
- Delorme, A. & Makeig, S. (2004) EEGLAB: an open source toolbox for analysis of single-trial EEG dynamics including independent component analysis. *J. Neurosci. Meth.*, **134**, 9–21.
- Donchin, E. & Coles, M.G. (1988) Is the P300 component a manifestation of context updating? *Behav. Brain Sci.*, **11**, 357–374.
- Duncan-Johnson, C.C. (1981) Young Psychophysicologist Award address, 1980. P300 latency: a new metric of information processing. *Psychophysiology*, **18**, 207–215.
- Duncan-Johnson, C.C. & Donchin, E. (1977) On quantifying surprise: the variation of event-related potentials with subjective probability. *Psychophysiology*, **14**, 456–467.
- Fabiani, M., Karis, D. & Donchin, E. (1986) P300 and recall in an incidental memory paradigm. *Psychophysiology*, **23**, 298–308.
- Friedman, D., Hakerem, G., Sutton, S. & Fleiss, J.L. (1973) Effect of stimulus uncertainty on the pupillary dilation response and the vertex evoked potential. *Electroen. Clin. Neuro.*, **34**, 475–484.
- de Gee, J.W., Knapen, T. & Donner, T.H. (2014) Decision-related pupil dilation reflects upcoming choice and individual bias. *Proc. Natl. Acad. Sci. USA*, **111**, E618–E625.
- Glover, A., Ghilardi, M.F., Bodis-Wollner, I. & Onofrij, M. (1988) Alterations in event-related potentials (ERPs) of MPTP-treated monkeys. *Electroen. Clin. Neuro.*, **71**, 461–468.
- Gold, J.I. & Shadlen, M.N. (2007) The neural basis of decision making. *Annu. Rev. Neurosci.*, **30**, 535–574.
- Hillyard, S.A., Squires, K.C., Bauer, J.W. & Lindsay, P.H. (1971) Evoked potential correlates of auditory signal detection. *Science*, **172**, 1357–1360.
- Kayser, J. & Tenke, C.E. (2006) Principal components analysis of Laplacian waveforms as a generic method for identifying ERP generator patterns: I. Evaluation with auditory oddball tasks. *Clin. Neurophysiol.*, **117**, 348–368.
- Keil, A., Bradley, M.M., Hauk, O., Rockstroh, B., Elbert, T. & Lang, P.J. (2002) Large-scale neural correlates of affective picture processing. *Psychophysiology*, **39**, 641–649.
- Kelly, S.P. & O'Connell, R.G. (2013) Internal and external influences on the rate of sensory evidence accumulation in the human brain. *J. Neurosci.*, **33**, 19434–19441.
- Kelly, S.P. & O'Connell, R.G. (2015) The neural processes underlying perceptual decision making in humans: recent progress and future directions. *J. Physiology-Paris*, **109**, 27–37.
- Kiani, R. & Shadlen, M.N. (2009) Representation of confidence associated with a decision by neurons in the parietal cortex. *Science*, **324**, 759–764.
- Kok, A. (2001) On the utility of P3 amplitude as a measure of processing capacity. *Psychophysiology*, **38**, 557–577.
- Kutas, M., McCarthy, G. & Donchin, E. (1977) Augmenting mental chronometry: the P300 as a measure of stimulus evaluation time. *Science*, **197**, 792–795.
- Link, S. & Heath, R. (1975) A sequential theory of psychological discrimination. *Psychometrika*, **40**, 77–105.
- Mars, R.B., Debener, S., Gladwin, T.E., Harrison, L.M., Haggard, P., Rothwell, J.C. & Bestmann, S. (2008) Trial-by-trial fluctuations in the event-related electroencephalogram reflect dynamic changes in the degree of surprise. *J. Neurosci.*, **28**, 12539–12545.
- Mavrogiorgou, P., Juckel, G., Frodl, T., Gallinat, J., Hauke, W., Zaudig, M., Dammann, G., Moller, H.J. & Hegerl, U. (2002) P300 subcomponents in obsessive-compulsive disorder. *J. Psychiatr. Res.*, **36**, 399–406.
- Mazurek, M.E., Roitman, J.D., Ditterich, J. & Shadlen, M.N. (2003) A role for neural integrators in perceptual decision making. *Cereb. Cortex*, **13**, 1257–1269.
- Murphy, P.R., Robertson, I.H., Balsters, J.H. & O'Connell, R.G. (2011) Pupilometry and P3 index the locus coeruleus–noradrenergic arousal function in humans. *Psychophysiology*, **48**, 1532–1543.
- Nieuwenhuis, S., Aston-Jones, G. & Cohen, J.D. (2005) Decision making, the P3, and the locus coeruleus–norepinephrine system. *Psychol. Bull.*, **131**, 510–532.
- Nieuwenhuis, S., De Geus, E.J. & Aston-Jones, G. (2011) The anatomical and functional relationship between the P3 and autonomic components of the orienting response. *Psychophysiology*, **48**, 162–175.
- Nolan, H., Butler, J.S., Whelan, R., Foxe, J.J., Bulthoff, H.H. & Reilly, R.B. (2012) Neural correlates of oddball detection in self-motion heading: a high-density event-related potential study of vestibular integration. *Exp. Brain Res.*, **219**, 1–11.

- O'Connell, R.G., Dockree, P.M. & Kelly, S.P. (2012) A supramodal accumulation-to-bound signal that determines perceptual decisions in humans. *Nat. Neurosci.*, **15**, 1729–1735.
- Palmer, J., Huk, A.C. & Shadlen, M.N. (2005) The effect of stimulus strength on the speed and accuracy of a perceptual decision. *J. Vision*, **5**, 1.
- Pineda, J. & Westerfield, M. (1993) Monkey P3 in an “oddball” paradigm: pharmacological support for multiple neural sources. *Brain Res. Bull.*, **31**, 689–696.
- Pineda, J., Westerfield, M., Kronenberg, B. & Kubrin, J. (1997) Human and monkey P3-like responses in a mixed modality paradigm: effects of context and context-dependent noradrenergic influences. *Int. J. Psychophysiol.*, **27**, 223–240.
- Polich, J. (2007) Updating P300: an integrative theory of P3a and P3b. *Clin. Neurophysiol.*, **118**, 2128–2148.
- Polich, J. & Criado, J.R. (2006) Neuropsychology and neuropharmacology of P3a and P3b. *Int. J. Psychophysiol.*, **60**, 172–185.
- Polich, J., Ladish, C. & Bloom, F.E. (1990) P300 assessment of early Alzheimer's disease. *Electroen. Clin. Neuro.*, **77**, 179–189.
- Prox, V., Dietrich, D.E., Zhang, Y., Emrich, H.M. & Ohlmeier, M.D. (2007) Attentional processing in adults with ADHD as reflected by event-related potentials. *Neurosci. Lett.*, **419**, 236–241.
- Ratcliff, R. & McKoon, G. (2008) The diffusion decision model: theory and data for two-choice decision tasks. *Neural Comput.*, **20**, 873–922.
- Reddi, B. & Carpenter, R. (2000) The influence of urgency on decision time. *Nat. Neurosci.*, **3**, 827–830.
- Resulaj, A., Kiani, R., Wolpert, D.M. & Shadlen, M.N. (2009) Changes of mind in decision-making. *Nature*, **461**, 263–266.
- Rohrbaugh, J.W., Donchin, E. & Eriksen, C.W. (1974) Decision making and the P300 component of the cortical evoked response. *Percept. Psychophys.*, **15**, 368–374.
- Santosh, P.J., Malhotra, S., Raghunathan, M. & Mehra, Y.N. (1994) A study of P300 in melancholic depression—correlation with psychotic features. *Biol. Psychiat.*, **35**, 474–479.
- Shadlen, M.N. & Kiani, R. (2013) Decision making as a window on cognition. *Neuron*, **80**, 791–806.
- Smith, D.B., Donchin, E., Cohen, L. & Starr, A. (1970) Auditory averaged evoked potentials in man during selective binaural listening. *Electroen. Clin. Neuro.*, **28**, 146–152.
- Smith, P.L. & Ratcliff, R. (2004) Psychology and neurobiology of simple decisions. *Trends Neurosci.*, **27**, 161–168.
- Smith, P.L. & Vickers, D. (1988) The accumulator model of two-choice discrimination. *J. Math. Psychol.*, **32**, 135–168.
- Squires, K.C., Hillyard, S.A. & Lindsay, P.H. (1973) Vertex potentials evoked during auditory signal detection: relation to decision criteria. *Percept. Psychophys.*, **14**, 265–272.
- Sutton, S., Braren, M., Zubin, J. & John, E. (1965) Evoked-potential correlates of stimulus uncertainty. *Science*, **150**, 1187–1188.
- Swick, D., Pineda, J. & Foote, S. (1994) Effects of systemic clonidine on auditory event-related potentials in squirrel monkeys. *Brain Res. Bull.*, **33**, 79–86.
- Urai, A.E. & Pfeffer, T. (2014) An Action-Independent Signature of Perceptual Choice in the Human Brain. *J. Neurosci.*, **34**, 5081–5082.
- Vandekerckhove, J. & Tuerlinckx, F. (2008) Diffusion model analysis with MATLAB: a DMAT primer. *Behav. Res. Methods*, **40**, 61–72.
- Verleger, R. (1988) Event-related potentials and cognition: a critique of the context updating hypothesis and an alternative interpretation of P3. *Behav. Brain Sci.*, **11**, 343–356.
- Verleger, R., Schroll, H. & Hamker, F.H. (2013) The unstable bridge from stimulus processing to correct responding in Parkinson's disease. *Neuropsychologia*, **51**, 2512–2525.
- Yeung, N. & Summerfield, C. (2012) Metacognition in human decision-making: confidence and error monitoring. *Philos. T. Roy. Soc. B.*, **367**, 1310–1321.